Elucidating the K-Edge X-Ray Absorption Near-Edge Structure of Cobalt Carbide

José G. Moya-Cancino,[a] Ari-Pekka Honkanen,[b] Ad M. J. van der Eerden,[a] Herrick Schaink,[a] Lieven Folkertsma,[a] Mahnaz Ghiasi,[a] Alessandro Longo,[c, d] Florian Meirer,[a] Frank M. F. de Groot,[a] Simo Huotari,*[b] and Bert M. Weckhuysen*[a]

The cobalt K-edge X-ray absorption near-edge structure of a cobalt carbide compound, synthetized under *in-situ* conditions, has been determined by using laboratory-based and synchrotron-based X-ray absorption spectroscopy. We have carburized pure cobalt metal *in-situ*, avoiding all adverse effects of metal-support interactions as well as any degradation of the cobalt carbide formed. A non-negative matrix factorization was applied to determine the features of the spectrum of cobalt carbide, highly needed to identify this phase in an unambiguous manner in cobalt-based Fischer-Tropsch catalysts.

Introduction

Fischer-Tropsch synthesis (FTS) is a hydrogenation reaction wherein a mixture of hydrogen and carbon monoxide, often named syngas, is converted into different hydrocarbon chains by a catalytic surface polymerization reaction.[1] The FTS reaction has become one of the most attractive technologies to produce ultra-clean synthetic fuels, most often being driven with cobalt-based catalysts because of the superior products characteristics as well as the high overall stability and low water-gas shift (WGS) activity.[2–6]

Despite more than 80 years of FTS research, one of the main remaining limitations in this catalytic technology is the gradual deactivation of the catalyst material over time, which is very costly given that the solid catalyst has to be regenerated and eventually replaced. Preventing catalyst deactivation has proven to be difficult given the fact that the precise mechanisms for catalyst deactivation are still under debate. Different

deactivation routes have been proposed, including the formation and deposition of coke on the active sites of the catalyst,[5,7] re-oxidation of the cobalt nanoparticles,[1,7] as well as the formation of inactive cobalt species, related to the existence of a Strong Metal-Support Interaction (SMSI) effect.[1,7,8] Especially the role of the formation of cobalt carbide during the FTS reaction remains highly controversial. Some studies relate its formation to the deactivation of the catalyst,[5,9,10] while others link Co carbide formation to a high selectivity to lower olefins at mild reaction conditions,[11,13] and to being an intermediate of the FTS reaction.[12] Definitive proofs for the role of cobalt carbides in FTS has yet not been provided, partly because of the difficulty to perform *in-situ* experiments that can correlate the formation of cobalt carbide with the performance of the reaction.[10–15] Standard experiments fail in unambiguously identifying the carbide species; X-ray Diffraction (XRD) for example is not very sensitive to the (possibly amorphous) cobalt carbide phases, while all *ex-situ* experiments may be unreliable because of the chemical instability of cobalt carbide in the absence of reaction conditions.

X-ray absorption spectroscopy techniques, on the other hand, are element-specific and able to probe the local structure around and the valence state of Co in the catalyst. They have been extensively used in the study of different catalytic systems using synchrotron radiation.[16–23] In the case of the identification of cobalt carbide formation, some *ex-situ* research has been reported.[15,24] Particularly interesting is the study performed by Singh *et al.*,[25] where a Co_2C spectrum acquired at *in-situ* conditions was reported. Among the different X-ray spectroscopies, X-ray Absorption Near-Edge Structure (XANES) is particularly attractive because it allows to perform studies under *in-situ*[6] and *ex-situ*[26] conditions in a laboratory- and synchrotron-based facility.

Here, we present a study focused on obtaining the Co K-edge spectrum of the elusive pure cobalt carbide, by performing the *in-situ* carburization reaction of pure metallic cobalt. Our purpose is to provide the reference spectrum of the cobalt carbide phase formed under *in-situ* FTS conditions of temperature and pressure, and simultaneously determine its spectro-

[a] J. G. Moya-Cancino, A. M. J. van der Eerden, H. Schaink, L. Folkertsma, Dr. M. Ghiasi, Dr. F. Meirer, Prof. Dr. F. M. F. de Groot, Prof. Dr. B. M. Weckhuysen
Inorganic Chemistry and Catalysis
Debye Institute for Nanomaterials Science
Utrecht University
Universiteitsweg 99, 3584 CG Utrecht (The Netherlands)
E-mail: b.m.weckhuysen@uu.nl

[b] A.-P. Honkanen, Prof. Dr. S. Huotari
Department of Physics
University of Helsinki
PO Box 64, 00014 Helsinki (Finland)
E-mail: simo.huotari@helsinki.fi

[c] Dr. A. Longo
Dutch-Belgian Beamline BM26
European Synchrotron Radiation (ESRF) Facility
CS 40220, 38043 Grenoble Cedex 9 (France)

[d] Dr. A. Longo
Istituto per lo Studio dei Materiali Nanostrutturati (ISMN)-CNR, USO
Via Ugo La Malfa, 153, 90146 Palermo (Italy)

scopic fingerprint, that is, the X-ray absorption fine structure of the pure Co carbide phase. By performing this study, we unambiguously establish the pure cobalt carbide spectrum, which can be used to unravel the real role of cobalt carbide phase during FTS reaction. By using the spectrum obtained, will be possible to unequivocally detect and quantify the formation of Co_2C during FTS reaction at *operando* conditions, and relate its formation with the deactivation of the catalyst material or either the olefin selectivity. Figure 1 shows a schematic of the methodology utilized in this research.
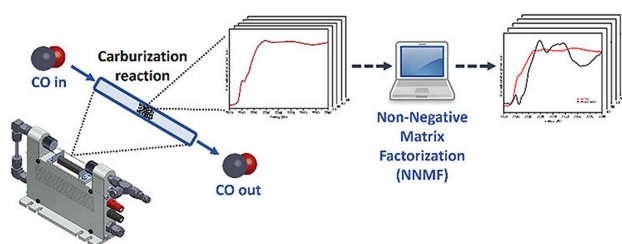

Figure 1. Schematic of the methodology used for the different carburization reaction experiments to make and later on identify a pure cobalt carbide phase with K-edge X-ray absorption near edge spectroscopy.

Results and Discussion

Two different experimental approaches were used for this research, laboratory-based, which allows to perform long-term carburization reactions, and synchrotron-based XANES, the first at the University of Helsinki, Finland,[27] and the latter at the BM26 (DUBBLE) beamline of the European Synchrotron Radiation Facility (ESRF).[6]

Figure 2 presents the different *in-situ* spectra acquired at different reaction times. Figure 2.I and Figure 2.II correspond to the experiments performed using the XANES laboratory-based set-up, while the experiment completed at BM26 beamline at ESRF is presented in Figure 2.III. The fully reduced (first) spectrum, in green, is contrasted to the spectra recorded at each time stamp, to visualize the variations in the pre-edge during evolving carburization. The most significant changes observed during the reaction are present in the pre-edge region. Figure 3 presents the difference of the cobalt reduced spectra and at different steps of the carburization reaction. In all experiments the observed changes are similar; differences arise from the different relative amount of cobalt carbides formed
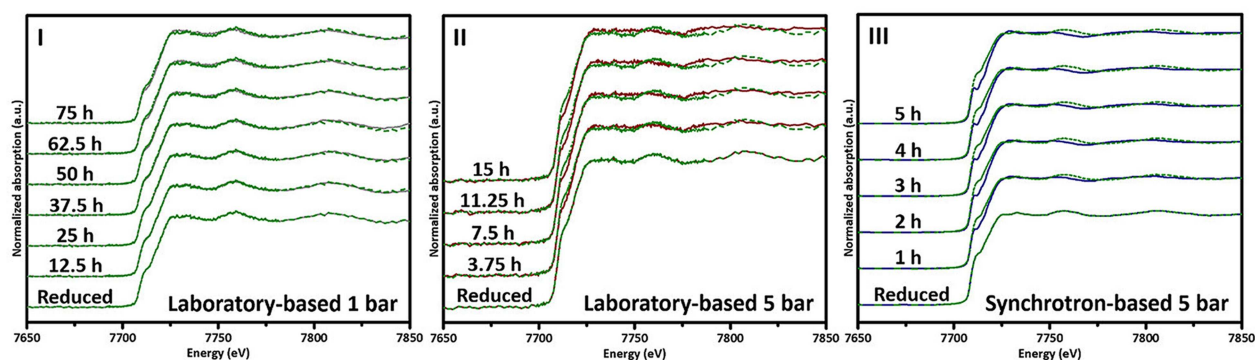

Figure 2. Co K-edge X-ray absorption near edge spectra at different steps of the carburization reaction of cobalt metal: I) laboratory-based measurements at 1 bar, II) laboratory-based measurements at 5 bar and III) synchrotron-based measurements at 5 bar. The green dashed spectra point out the reduced spectra and was used to visualize the change of the spectra over time.
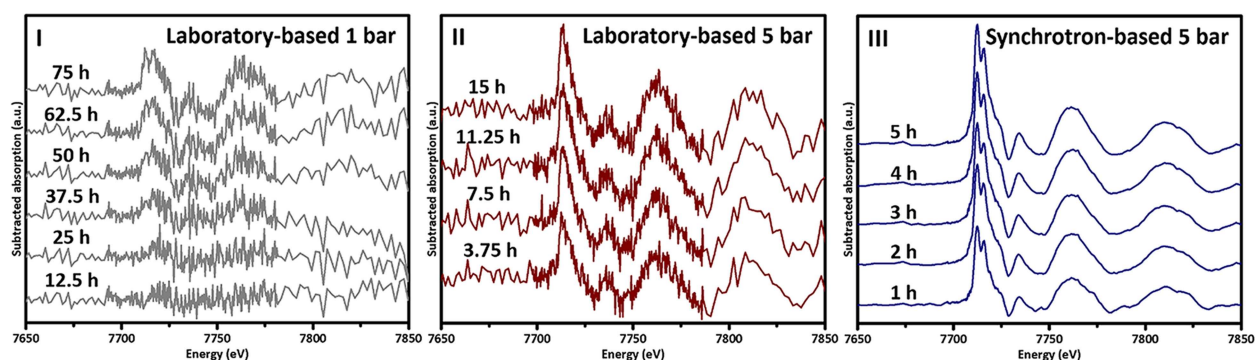

Figure 3. Difference between the Co K edge X-ray absorption near edge spectra of reduced (metallic) and at different steps of the carburization reaction: I) laboratory-based measurements at 1 bar, II) laboratory-based measurements at 5 bar and III) synchrotron-based measurements at 5 bar.

due to the different reaction conditions (pressure and CO flow rate).

To determine the effect of the differences in the energy resolution from the laboratory-based and synchrotron-based experiments, Co foil reference samples measured using the lab-based spectrometer and ESRF were contrasted, as shown in Figure S1. It was established that the energy resolution is reasonably comparable for both set-ups and does not play a significant role in the quality of the data acquired.

Next, Non-Negative Matrix Factorization (NNMF)[28] was applied to the spectra of the carburized samples taken at different reaction times, namely after 75 h, 15 h and 5 h, to deconvolute the XANES into two pure contributing components. By using the NNMF method it is possible to determine the contribution of Co_2C to the carburized spectrum as there is no other cobalt species presents in the sample apart from metallic cobalt and cobalt carbide (details of this approach and the results obtained from NNMF of the data matrix for the different experiments performed, laboratory-based and SR-based measurements can be found in section S2 of the Supplementary Information (SI)).

Additionally, a simulation of the XANES spectrum, based on the crystalline structure of Co_2C, was performed using the FDMNES and FEFF9 programs[29,30] to corroborate the results obtained from the NNMF calculations. The structure of Co_2C was obtained from the Crystallography Open Database, entry ID 1528415.[31] The structure given as input to the simulations had the space group Pmnn, with lattice parameters a = 2.8969 Å, b = 4.4465 Å, c = 4.3707 Å, $\alpha = \beta = \gamma = 90°$. The most important detail of the simulation performed by FDMNES was the size of the cluster where final state calculation was performed, R = 7.0 Å. FEFF 9.6.4 was used in reciprocal space and the k-point grid was converged at 200 k-points. The NNMF results from laboratory- and synchrotron-based measurements at 5 bar and the different simulations are shown in Figure 4.
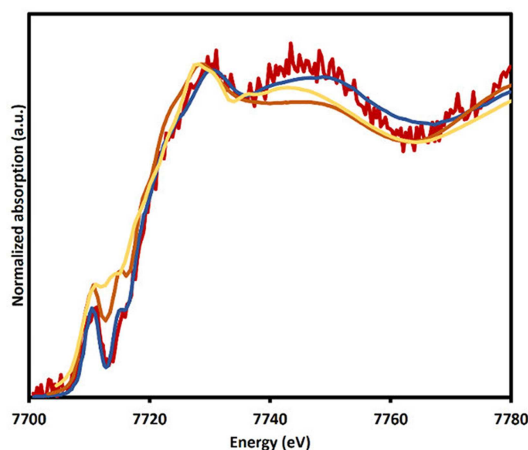

Figure 4. Simulated X-ray absorption near edge spectrum of cobalt carbide (Co_2C) using the FDMNES and FEFF9 programs. The simulated FDMNES and FEFF9 spectrum are indicated in orange and yellow, respectively, while the results from non-negative matrix factorization (NNMF) of the synchrotron-based data measured at 5 bar are indicated in blue, and for the laboratory-based data measured at 5 bar are indicated in red.

All Co K-edge XANES spectra, experimental and theoretical, obtained for Co_2C agree with each other in the following terms: there are two pre-edges; one at 7710 eV and the second at 7714 eV, which correspond to the quadrupole 1s-3d and nonlocal dipolar Co—C—Co 1s-2p-3d transitions, respectively, as analyzed in detail, i.e., for $LiCoO_2$.[32,33] And, there is a white line peak at 7729 eV. The results are in good agreement with the spectrum proposed by Singh et al.[25] (Figure S2.23).

Using the in-situ carburization method, problems such as the degradation of the cobalt carbides into cobalt metallic and graphite[10] and the subsequent oxidation of the metallic cobalt into CoO and Co_3O_4 can be avoided, which represents an advantage over the ex-situ characterization methods previously reported in literature.[15,24]

Conclusions

We have developed a methodology that allows to determine the main features of the K-edge X-ray absorption near edge structure of cobalt carbide, which is of importance for elucidating the activation and deactivation processes taking place in cobalt-based Fischer-Tropsch synthesis catalysts. By using two distinct experimental approaches, making use of lab- and synchrotron-based methods, it was possible to measure the Co X-ray absorption K-edge spectrum during the carburization reaction of pure metallic cobalt under different in-situ reaction conditions, i.e. at atmospheric and elevated pressures. NNMF was applied to obtain a pure Co_2C spectrum, which was further corroborated by theoretical calculations. The developed methodology is also useful and more generally applicable for the identification of phase-pure X-ray absorption spectra of distinct metal oxides, carbides and nitrides within more complex solid catalyst materials.

Experimental Section

For the in-situ synthesis of cobalt carbide we have used the approach, as proposed by Claeys et al. and Cats et al.,[10,34] which requires a complete reduction of Co_3O_4 to Co metallic followed by the carburization of the sample in a pure flow of CO (Figure S3). The in-situ reactor set-up used has been introduced in our previous study.[6] In short, the reactor is made of a quartz capillary with an outer diameter of 1 mm, wherein the temperature is controlled by a thermocouple positioned in the bed of the reactor (Figure S4). To test our experimental procedure and obtain data about the cobalt carbide formation at different thermodynamic parameters, different in-situ experiments were done at 523 K, and CO flow of 1 ml/min. The differences in the experiments were the pressure and duration of the reaction: 1 bar, duration 75 h; and 5 bar, duration 15 h. In this way, we obtained data on the dependence of the cobalt carbide formation rate as a function of pressure. The laboratory-based XANES spectrometer used for this work[6,27,35] employs the Bremsstrahlungs spectrum in the 4–20 keV photon energy range emitted by an Ag-tube used as X-ray source and operated at a current of 40 mA and a voltage of 20 kV. Further, a Si (533) spherically bent crystal monochromator utilizing the Johann geometry with a bending radius R = 0.5 m, and a NaI scintillator detector were employed. All these components (source, mono-

chromator, detector) are arranged on the Rowland circle. To get corroborative data using a synchrotron light source, we also performed *in-situ* X-ray absorption near edge structure (XANES) measurements at the beamline BM26 (DUBBLE) of ESRF (Grenoble, France), using 523 K, 5 bar, and a CO flow of 5 ml/min. The purpose of performing the synchrotron experiment was to obtain data to support and confirm the ones obtained at the small-scale laboratory-based set-up. The *in-situ* XANES data were compared to data from *ex-situ* XANES measurements of Co reference materials: Co_3O_4 (Sigma-Aldrich, 99.5%), CoO (Acros Organics, 99+%) and Co (Co foil, 99.9%). These data are shown in Figure S5. The *in-situ* carburization reactions were divided in two different steps: a) activation (reduction of the pure Co_3O_4 to Co^0) at 673 K and 1 bar, in a pure H_2 flow (AGA, $H_2 > 99.999\%$, and Air Liquid, $H_2 > 99.995\%$) and b) carburization reaction at 523 K, 1 and 5 bar in a pure CO flow (AGA, CO $> 99.97\%$, and Air Liquid, CO $> 99.997\%$). Before starting the activation stage, a Co spectrum was collected to single out the oxidation state of the cobalt samples. During the execution of the different carburization experiments, the different spectra were collected continuously. The temperature profile designed for the experiments considered the raising of the temperature from room temperature (RT) to 673 K using a heating rate of 5 K/min, keeping the temperature at 673 K for 1–4 h (leading to a complete reduction of cobalt). Once the cobalt was completely reduced into its metallic state, the temperature was decreased to 523 K with a rate of 5 K/min and the gas was switched to CO in the case of the carburization reaction at 1 bar; and in the case of the carburization experiments at 5 bar, the temperature was reduced to RT, the system was pressurized to 5 bar on a CO atmosphere, and the temperature was increased to 523 K with a rate of 5 K/min. The carburization reaction at 1 bar was complete after 75 h (for the laboratory-based experiments), and the carburization reactions at 5 bar were completed after 15 h (for the laboratory-based experiments) and 5 h (for the synchrotron-based experiments).

Acknowledgements

Conflict of Interest

The authors declare no conflict of interest.

[1] A. Y. Khodakov, W. Chu, P. Fongarland, *Chem. Rev.* **2007**, *107*, 1692–1744.
[2] M. Bremaud, P. Fongarland, J. Anfray, S. Jallais, D. Schweich, A. Y. Khodakov, *Catal. Today* **2005**, *106*, 137–142.
[3] E. de Smit, B. M. Weckhuysen, *Chem. Soc. Rev.* **2008**, *37*, 2758–2781.
[4] T. O. Eschemann, J. Oenema, K. P. de Jong, *Catal. Today* **2016**, *261*, 60–66.
[5] A. Carvalho, V. V. Ordomsky, Y. Luo, M. Marinova, A. R. Muniz, N. R. Marcilio, A. Y. Khodakov, *J. Catal.* **2016**, *344*, 669–679.
[6] J. G. Moya-Cancino, A.-P. Honkanen, A. M. J. van der Eerden, H. Schaink, L. Folkertsma, M. Ghiasi, A. Longo, F. M. F. de Groot, F. Meirer, S. Huotari, B. M. Weckhuysen, *ChemCatChem* **2019**, *11*, 1039–1044.
[7] N. E. Tsakoumis, M. Rønning, Ø. Borg, E. Rytter, A. Holmen, *Catal. Today* **2010**, *154*, 162–182.
[8] A. Carvalho, V. V. Ordomsky, Y. Luo, M. Marinova, A. R. Muniz, N. R. Marcilio, A. Y. Khodakov, *J. Catal.* **2016**, *344*, 669–679.
[9] Y.-H. Zhao, H.-Y. Su, K. Sun, J. Liu, W.-X. Li, *Surf. Sci.* **2012**, *606*, 598–604.
[10] M. Claeys, M. E. Dry, E. van Steen, E. du Plessis, P. J. van Berge, A. M. Saib, D. J. Moodley, *J. Catal.* **2014**, *318*, 193–202.
[11] L. Zhong, F. Yu, Y. An, Y. Zhao, Y. Sun, Z. Li, T. Lin, Y. Lin, X. Qi, Y. Dai, L. Gu, J. Hu, S. Jin, Q. Shen, H. Wang, *Nature* **2016**, *538*, 84–87.
[12] W. Chen, I. A. W. Filot, R. Pestman, E. J. M. Hensen, *ACS Catal.* **2017**, *7*, 8061–8071.
[13] Y. Xiang, N. Kruse, *Nat. Commun.* **2016**, *7*, 13058.
[14] J. Cheng, P. Hu, P. Ellis, S. French, G. Kelly, C. M. Lok, *J. Phys. Chem. C* **2010**, *114*, 1085–1093.
[15] J. C. Mohandas, M. K. Gnanamani, G. Jacobs, W. Ma, Y. Ji, S. Khalid, B. H. Davis, *ACS Catal.* **2011**, *1*, 1581–1588.
[16] S. Bordiga, E. Groppo, G. Agostini, J. A. van Bokhoven, C. Lamberti, *Chem. Rev.* **2013**, *113*, 1736–1850.
[17] G. Jacobs, P. M. Patterson, Y. Zhang, T. Das, J. Li, B. H. Davis, *Appl. Catal. A* **2002**, *233*, 215–226.
[18] G. Jacobs, T. K. Das, P. M. Patterson, J. Li, L. Sanchez, B. H. Davis, *Appl. Catal. A* **2003**, *247*, 335–343.
[19] T. K. Das, G. Jacobs, P. M. Patterson, W. A. Conner, J. Li, B. H. Davis, *Fuel* **2003**, *82*, 805–815.
[20] G. Jacobs, J. A. Chaney, P. M. Patterson, T. K. Das, B. H. Davis, *Appl. Catal. A* **2004**, *264*, 203–212.
[21] G. Jacobs, Y. Ji, B. H. Davis, D. Cronauer, J. Kropf and C. L. Marshall, *Appl. Catal. A* **2007**, *333*, 177–191.
[22] A. M. Beale, S. D. M. Jacques, B. M. Weckhuysen, *Chem. Soc. Rev.* **2010**, *39*, 4656–4672.
[23] F. Meirer, B. M. Weckhuysen, *Nat. Rev. Mater.* **2018**, *3*, 324–340.
[24] G. Kwak, M. H. Woo, S. C. Kang, H.-G. Park, Y.-J. Lee, K.-W. Jun, K.-S. Ha, *J. Catal.* **2013**, *307*, 27–36.
[25] J. A. Singh, A. S. Hoffman, J. Schumann, A. Boubnov, A. S. Asundi, S. S. Nathan, J. Nørskov, S. R. Bare, S. F. Bent, *ChemCatChem* **2019**, *11*, 799–809.
[26] S. K. Padamati, D. Angelone, A. Draksharapu, G. Primi, D. J. Martin, M. Tromp, M. Swart, W. R. Browne, *J. Am. Chem. Soc.* **2017**, *139*, 8718–8724.
[27] A.-P. Honkanen, S. Ollikkala, T. Ahopelto, A.-J. Kallio, M. Blomberg, S. Huotari, arXiv:1812.01075.
[28] C. J. Sahle, M. A. Schroer, I. Juurinen, J. Niskanen, *Phys. Chem. Chem. Phys.* **2016**, *18*, 16518–16526.
[29] O. Bunau, Y. Joly, *J. Phys. Condens. Matter* **2009**, *21*, 345501.
[30] J. J. Rehr, J. J. Kas, F. D. Vila, M. P. Prange, K. Jorissen, *Phys. Chem. Chem. Phys.* **2010**, *12*, 5503–5513.
[31] J. Clarke, K. H. Jack, *Chem. Ind.-Lond.* **1951**, *1951*, 1004.
[32] A. Juhin, F. M. F. de Groot, G. Vankó, M. Calandra, C. Brouder, *Phys. Rev. B* **2010**, *81*, 115115–115125.
[33] F. M. F. de Groot, G. Vankó, P. Glatzel, *J. Phys. Condens. Matter* **2009**, *21*, 104207–104213.
[34] K. H. Cats, B. M. Weckhuysen, *ChemCatChem* **2016**, *8*, 1531–1542.
[35] R. Bes, T. Ahopelto, A.-P. Honkanen, S. Huotari, G. Leinders, J. Pakarinen, K. Kvashnina, *J. Nucl. Mater.* **2018**, *507*, 50–53.